1990

Dynamics of Compliance Mechanisms in Scroll Compressors, Part I: Axial Compliance

J. J. Nieter
United Technologies Research Center

T. Barito
United Technologies Carrier

DYNAMICS OF COMPLIANCE MECHANISMS IN SCROLL COMPRESSORS
PART I: AXIAL COMPLIANCE

Jeff J. Nieter
Research Engineer
United Technologies Research Center
East Hartford, CT 06108

Tom Barito
Senior Engineer
United Technologies Carrier
Syracuse, NY 13221

ABSTRACT

In this paper an axial compliance mechanism in the form of a back chamber below the orbiting scroll is discussed for the scroll compressor. Pressurization of the back chamber is modeled as a dynamic process using mass and energy conservation in the back chamber along with compressible Fanno flow for predicting the highly oscillatory gas flow into or out of the back chamber through a supply line. The model is validated by comparison of the predicted back chamber pressures with dynamic pressure measurements. The effect of the dynamic pressure in the back chamber on scroll compressor performance over a wide range of geometries and operating conditions is discussed.

NOMENCLATURE

c_p	Specific heat capacity at constant pressure
d	Differential operator
D	Diameter
E	Energy
f	Friction factor at flow boundary
g	Gravitational acceleration
h	Enthalpy of gas
H_D	Hydraulic diameter
L	Length
m	Mass of gas
$\dot{m}$	Mass flow rate
p	Pressure
Δp	Peak-to-peak (p-p) pressure
$\dot{Q}$	Rate of heat transfer
SOC	Start of closed compression process
SOD	Start of discharge process
SOS	Start of suction process
t	Time
T	Temperature
U	Internal energy of gas
v	Velocity of gas
V	Volume
$\dot{W}$	Rate of boundary work
z	Elevation of gas
θ	Crank angle position of orbiting scroll
ρ	Density of gas

Subscripts

bc	Back chamber
cv	Control volume
in	Into control volume
out	Out of control volume
o	Reference pressure
sl	Supply line
up	Upstream of control volume

INTRODUCTION

Scroll compressors are quickly gaining popularity in many applications due to their high efficiency, fewer parts, and low noise and vibration as compared to competing compressor types. It is also widely recognized that in order to achieve high efficiency with a scroll compressor, some form of compliance mechanism is required. A compliance mechanism not only enables the scroll compressor to achieve acceptable performance levels, it also provides tolerance to solid contaminants and liquid slugs. Axial compliance is an approach utilized in many scroll compressors in the form of a back chamber which affects pressurization at the back side of the orbiting scroll and forces it against the fixed scroll. This insures that the axial clearances at the tips of the mating scroll wraps are minimized or eliminated, thus minimizing leakage across this sealing surface. The actuation of the orbiting scroll against the fixed scroll to close these tip clearances is shown in Fig. 1. Axial compliance also provides relief of high pressure during liquid ingestion as well as accommodating wear of material at the orbiter thrust surface. Further, it provides the opportunity to balance the axial gas forces on the orbiter to minimize the friction at the thrust surface. Several references[1-3] have discussed this method briefly in recent years. In this paper, a more detailed discussion of the analysis and effects of back chamber design will be given.

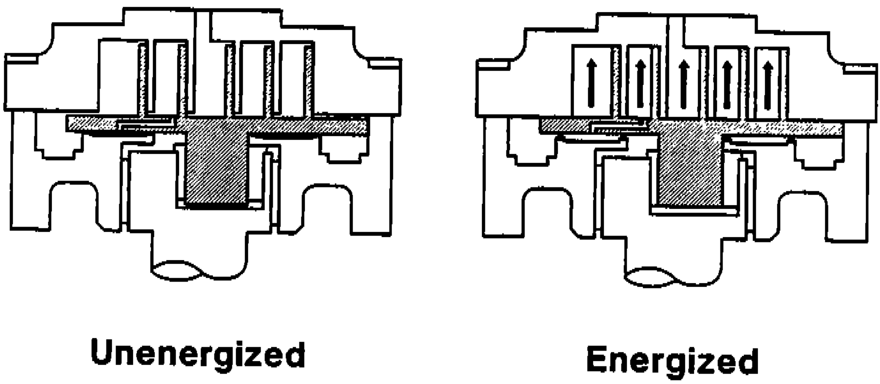

Figure 1 Actuation of back chamber axial compliance to minimize tip clearances

ANALYTICAL MODEL

The flow of gas into or out of the back chamber below the orbiting scroll is caused by the pressure difference between the back chamber and the supply port location in the compression chamber pockets. A schematic for the back chamber model is shown in Fig. 2 which identifies the important geometric parameters. The pressure history for a typical scroll compressor is shown in Fig. 3 where the pressure plotted is for the gas in a moving control volume which goes from the start of suction (SOS) to the start of closed compression (SOC) and on through start of discharge (SOD). The 360 deg. pressure range a supply port might be exposed to is indicated as well. It is evident from Fig. 3 that there can be a substantial variation in the pressure to which the supply port feeding the back chamber is exposed. Consequently, it is important to properly model the flow process through the supply lines.

The instantaneous mass flow rate of gas entering or leaving the back chamber control volume through a supply line is described using the Fanno model. This assumes steady, compressible, adiabatic flow of an ideal gas with boundary friction. It is important to account for the wall friction effects since a supply line will typically be very small in diameter to minimize the recirculation of flow from high pressure compression pockets into the back chamber and then out to lower pressure compression pockets during part of the cycle. Also, as we shall see later, a smaller diameter supply line will reduce pressure pulsations in the back chamber.

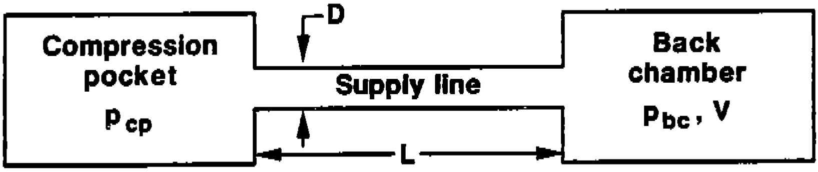

Figure 2 Schematic of back chamber model

The governing equations for Fanno flow are the following[4], based on conservation of mass, balance of energy, and balance of momentum, respectively:

$$d(\rho v) = 0 \tag{1}$$

$$c_p dT + d\left(\frac{v^2}{2}\right) = 0 \tag{2}$$

$$dp + f\left(\frac{\rho v^2}{2}\right)\frac{dz}{H_D} + (\rho v)dv = 0 \tag{3}$$

In modeling the back chamber pressurization process, the instantaneous mass of gas contained within the back chamber control volume is described by the differential continuity equation,

$$\frac{d}{dt}(m_{bc}) = \sum_i (\dot{m}_{sl})_i \tag{4}$$

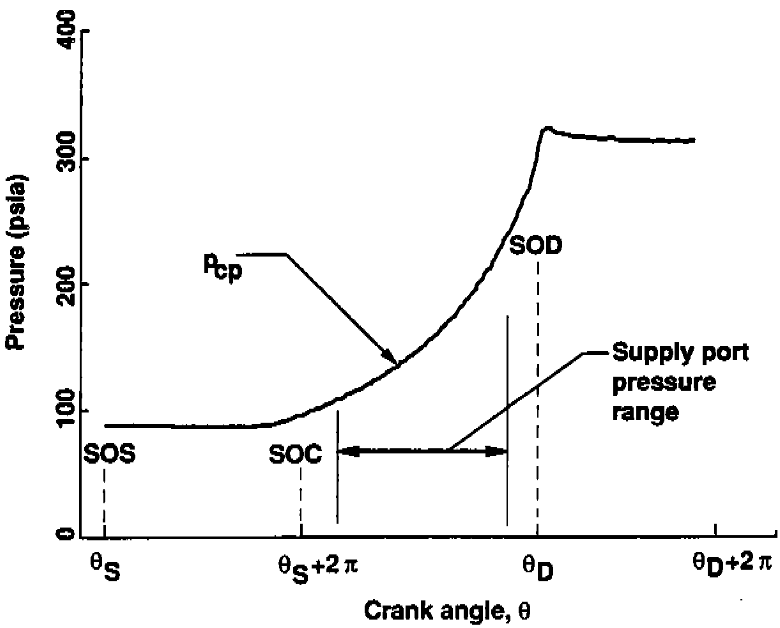

Figure 3 Typical pressure history for scroll compressor

where it is assumed that gas properties are uniform throughout the back chamber (this also applies to the compression chamber pockets).

The state of the gas in the back chamber can be described using the first law of thermodynamics on a time rate basis:

$$\frac{d}{dt}(E_{cv}) = \dot{Q} - \dot{W} + \Sigma\, \dot{m}_{in}[\, h + \frac{v^2}{2} + gz\,]_{in} - \Sigma\, \dot{m}_{out}[\, h + \frac{v^2}{2} + gz\,]_{out} \quad (5)$$

where it is assumed the terms for boundary work and kinetic and potential energies are negligible. Then the following equation remains to describe the energy balance on the back chamber:

$$\frac{d}{dt}(U_{bc}) = \dot{Q} + \sum_i (\dot{m}_{sl} h_{up})_i \quad (6)$$

where it is assumed the time rate change of energy in the control volume equals the time rate change of the internal energy of the gas.

The dynamic back chamber model described above predicts static and dynamic pressures very well and has been validated with data measured in a laboratory scroll compressor. The pressure measurements were obtained as shown in Fig. 4 where quartz piezoelectric transducers were used to measure peak-to-peak (p-p) pressure pulsations and a static pressure tap was used to measure the average pressure. The dynamic pressures were measured at three locations around the circumference of the back chamber to insure accuracy and to verify no spatial fluctuations occured throughout the chamber. Comparisons between measured and predicted back chamber pressures at various operating conditions and nominal 3500 rpm are shown in Fig. 5 for average pressure and in Fig. 6 for peak-to-peak pressure pulsation. In both figures, two predicted curves are plotted. As indicated, one curve was predicted assuming no oil film inside the supply line and used the machined line diameter and surface roughness. The other predicted curve assumed a thin oil film on the inside of the supply line and used a very small value for surface roughness. The comparisons in both figures show very good agreement.

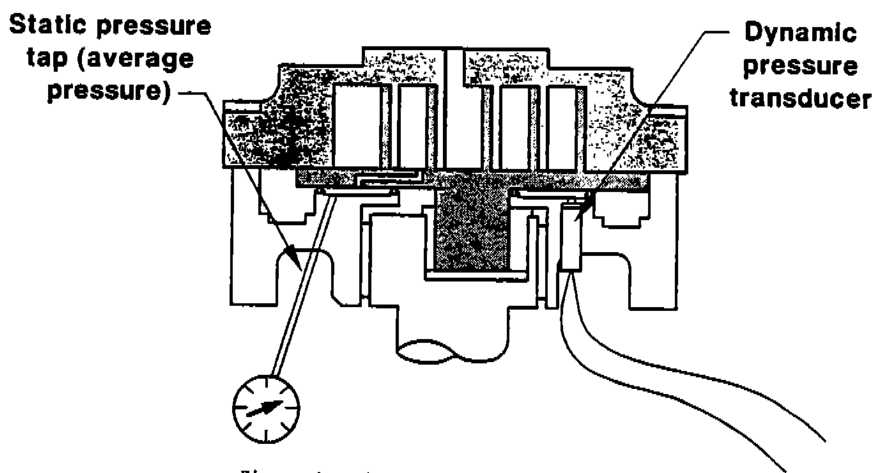

Figure 4 Schematic of instrumention

BACK CHAMBER DYNAMIC CHARACTERISTICS

In Fig. 7, the location of the supply port around the inside of the orbiter wrap is defined from the outer tip. Figure 8 shows how the pressure in the back chamber varies with this supply port location. As expected, the static and dynamic

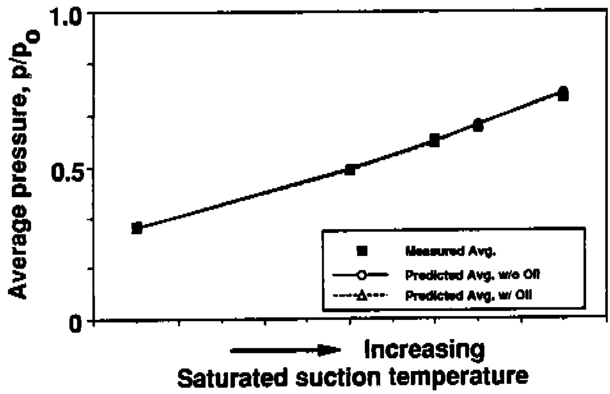

Figure 5 Comparison of measured and predicted average pressure in back chamber at 45/130/65 deg.F and nominal 3500 rpm

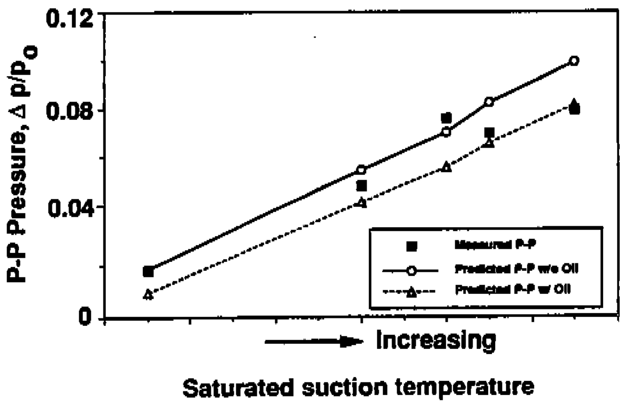

Figure 6 Comparison of measured and predicted peak-to-peak pressure in back chamber at 45/130/65 deg.F and nominal 3500 rpm

pressures increase as the port is moved further into the compression process for this operating condition. The average and peak-to-peak pressures plotted in Figs. 8 - 11 are for the 45/130/65 deg.F condition and 3500 rpm. In Fig. 9, the sensitivity of back chamber pressure to volume is shown. Clearly, use of a sufficiently large back chamber volume is important to avoid excessive pressure pulsations, however, too large of a volume results in the static pressure decreasing. Figure 10 shows that the back chamber pressure is also very sensitive to supply port and line diameter. A smaller diameter supply line will help reduce pressure pulsations, but will also reduce the average pressure substantially. In contrast, Fig. 11 indicates that the back chamber pressure is relatively insensitive to supply line length. The effect of different operating conditions on pressure pulsations in the back chamber is given in Fig. 12 and shows that for a given geometry, the pulsations are greatest for the condition with the greatest saturated suction temperature (and thus pressure). This result is consistent with the supply port location such that it is exposed to the closed compression process for most of the cycle.

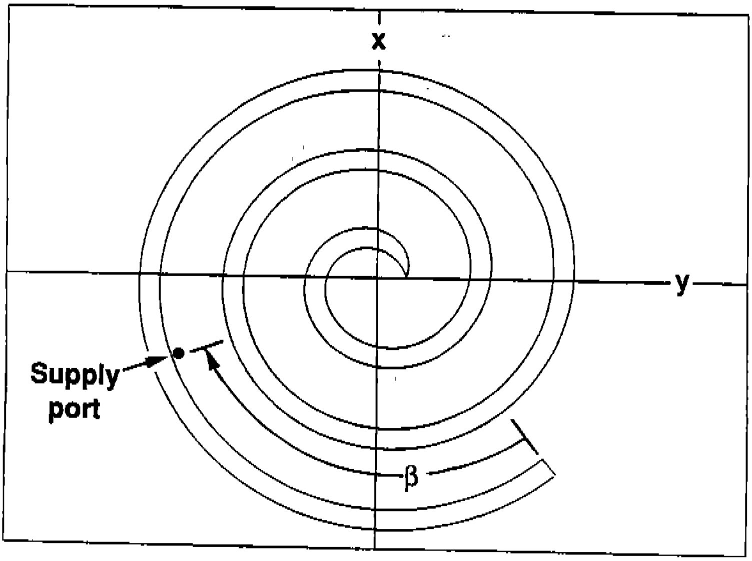

Figure 7 Description of back chamber supply port location

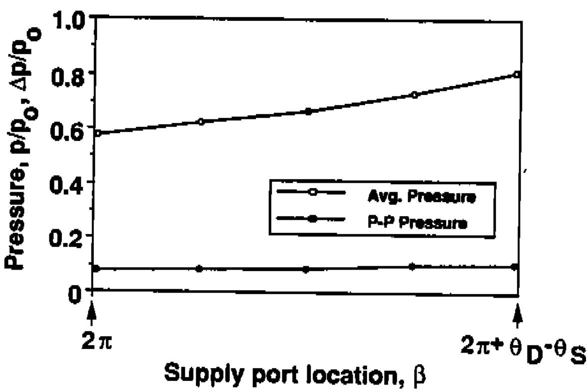

Figure 8 Effect of supply port location on back chamber pressure at 45/130/65 deg.F and 3500 rpm

Thus far the results shown were of back chamber pressure. The thermodynamic performance of the scroll compressor can be significantly effected by back chamber geometry as well[3]. In Fig. 13, the compression power required to compress the gas with various back chamber volumes is shown at the different operating conditions. The sensitivity is not terribly great, but nevertheless, the power required to compress the gas increases as the volume increases due to increased gas recirculation. This occurs because gas flows into the back chamber from high pressure compression pockets and subsequently during a cycle flows back to lower pressure pockets. In Fig. 14, the effect of back chamber volume on friction loss at the orbiter thrust surface is shown for the various operating conditions. The trend in these curves reflects the effect of back chamber volume on average pressure. Since the thrust force is directly dependent upon the pressure in the back chamber, and the back chamber pressure is effected by volume, it should not be surprising that friction loss at the thrust surface is effected by volume.

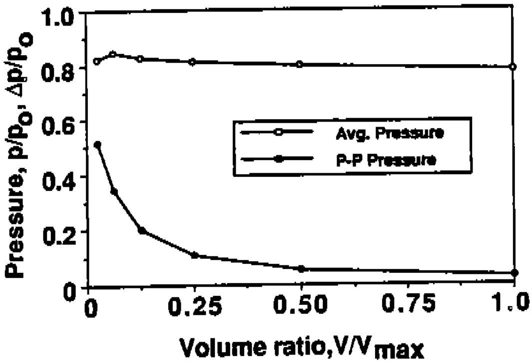

Figure 9 Effect of back chamber volume on back chamber pressure at 45/130/65 deg.F and 3500 rpm

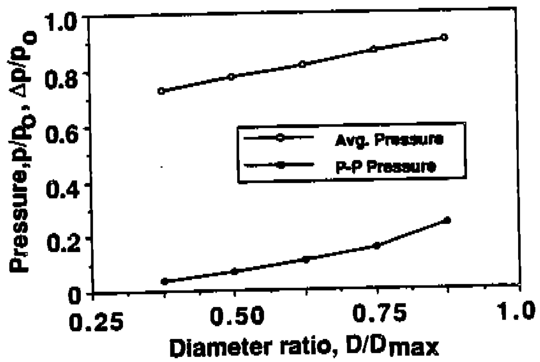

Figure 10 Effect of supply line diameter on back chamber pressure at 45/130/65 deg.F and 3500 rpm

CONCLUSIONS

A scroll compressor back chamber axial compliance model consisting of the differential continuity equation, the Fanno flow description, and the energy balance equation has been shown to predict back chamber pressures very well. The ability to predict these pressures is important to correctly analyze the forces and moments acting on the orbiting scroll. The interaction of the back chamber pressurization process with the scroll compression process has been accounted for as well. This analytical model is a useful tool for obtaining a back chamber design which causes the least amount of performance loss.

REFERENCES

1. Tojo, K., et al., "A SCROLL COMPRESSOR FOR AIR CONDITIONERS", Proc. of the 1984 Intern. Compr. Eng. Conf. (Purdue), July 1984, pp. 496-503.
2. Hayano, M., et al., "PERFORMANCE ANALYSIS OF SCROLL COMPRESSOR FOR AIR CONDITIONERS", Proc. of the 1986 Intern. Compr. Eng. Conf. (Purdue), Aug. 1986, pp. 856-871.
3. Tojo, K., et al., "COMPUTER MODELING OF SCROLL COMPRESSOR WITH SELF ADJUSTING BACK-PRESSURE MECHANISM", Proc. of the 1986 Intern. Compr. Eng. Conf. (Purdue), Aug. 1986, pp. 872-886.
4. Shames, I.H., MECHANICS OF FLUIDS, McGraw-Hill, 1962.

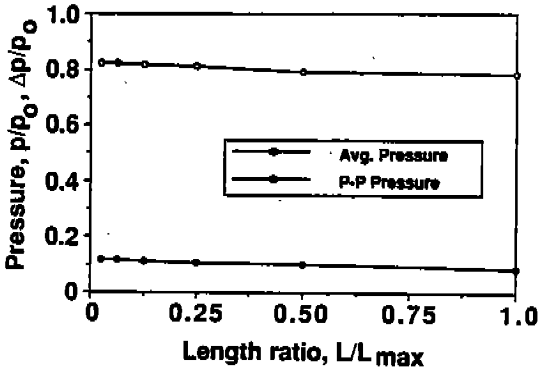

Figure 11 Effect of supply line length on back chamber pressure at 45/130/65 deg.F and 3500 rpm

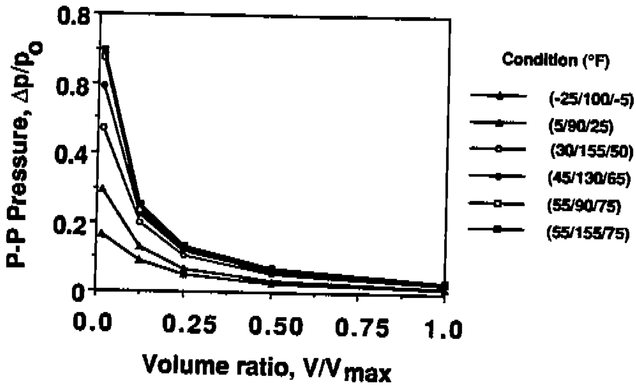

Figure 12 Effect of volume and operating condition on back chamber pressure pulsations at 3500 rpm

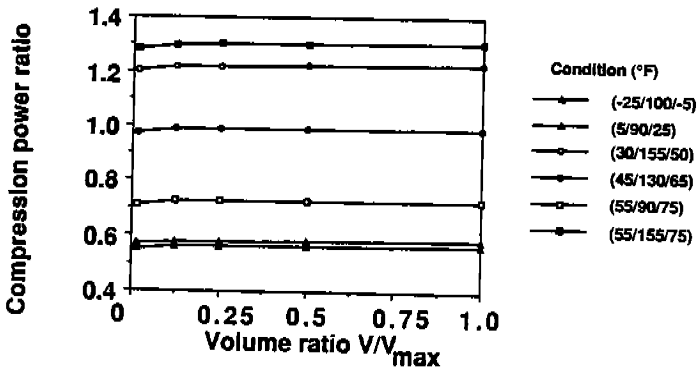

Figure 13 Effect of volume and operating condition on scroll compression power at 3500 rpm

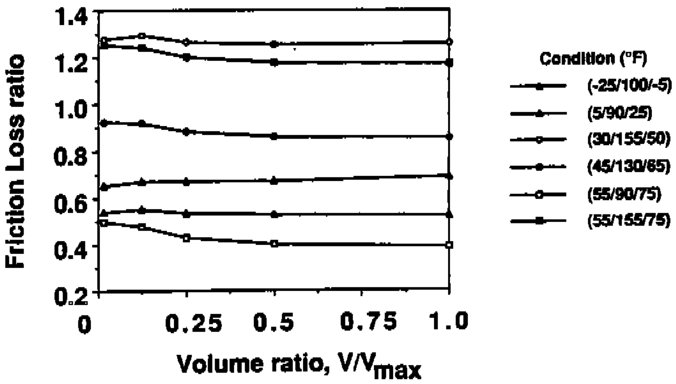

Figure 14 Effect of volume and operating condition on thrust surface friction loss at 3500 rpm